GLOBAL CLASSIFICATION OF MESSENGER SPECTRAL REFLECTANCE DATA AND A DETAILED LOOK AT RUDAKI PLAINS. Mario D'Amore (mario.damore@dlr.de)[1], Jörn Helbert[1], Alessandro Maturilli[1], James W. Head[2],Ann L. Sprague[3], Noam R. Izenberg[4], Gregory M. Holsclaw[5], William E. McClintock[5], Faith Vilas[6], and Sean C. Solomon[7]. [1]DLR, Rutherfordstrasse 2, Berlin, Germany; [2]Department of Geological Sciences, Brown University, Providence, RI 02912, USA. [3]Lunar and Planetary Laboratory, University of Arizona, Tucson, AZ 85721, USA; [4]The Johns Hopkins University Applied Physics Laboratory, Laurel, MD 20723, USA; [5]Laboratory for Atmospheric and Space Physics, University of Colorado, Boulder, CO 80303, USA; [6]Planetary Science Institute, Tucson, AZ 85719, USA; [7]Department of Terrestrial Magnetism, Carnegie Institution of Washington, Washington, DC 20015, USA.

Introduction: The MESSENGER spacecraft continues to provide new data that change our views on the nature of Mercury's surface. Under the hypothesis that surface compositional information can be efficiently derived from spectral reflectance measurements with the use of statistical techniques, we have employed unsupervised hierarchical clustering analyses to identify and characterize spectral units from observations made with MESSENGER's Mercury Atmospheric and Surface Composition Spectrometer (MASCS) instrument. This method proved successful on MASCS data obtained during MESSENGER's Mercury flybys even in the absence of a photometric correction.

MASCS: The MASCS instrument [1,2] consists of a small Cassegrain telescope with an aperture that simultaneously feeds an Ultraviolet and Visible Spectrometer (UVVS) and a Visible and Infrared Spectrograph (VIRS). VIRS is a fixed concave-grating spectrograph with a beam splitter that disperses the spectrum onto a 512-element silicon visible photodiode array and a 256-element indium-gallium-arsenide infrared photodiode array with a spectral resolution of 5 nm. VIRS has a circular field of view with a circular diameter of 0.023°. The visible (VIS) detector of VIRS covers the wavelength range from 300 to 1050 nm, and the near-infrared (NIR) detector covers the range 850-1450 nm. The study of Mercury's surface presented here uses only the VIRS channel of MASCS.

Data retrieval: To retrieve and characterize the number and spectral shapes of the different components present in the dataset (**Fig. 1**), we collected all MASCS observations to date (> 1.5×10^6 spectra). Because there are no photometric corrections for MASCS available yet, the data were normalized to the reflectance level at 700 nm, yielding a ratio nearly independent of incidence and emission angles. The data were then interpolated to a fixed spatial grid, averaging the sub-pixel spectra. The product is a map of reflectance ratio, along with error and frequency maps to address potential error in the process and to assess reliability. The output is essentially a geographically registered cube-image of averaged MASCS spectra on a constant spatial grid. The spatial grid resolution varies between 4 pixels per degree (ppd) for global analyses and 0.5 ppd

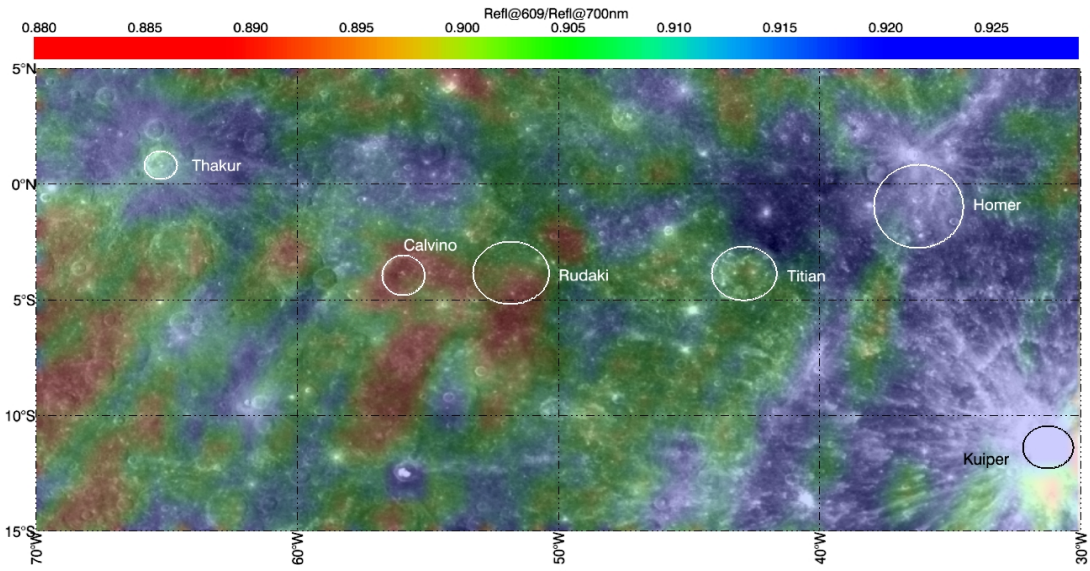

Fig. 1. Map of the ratio of reflectance at 609 nm to that at 700 nm as measured by MASCS in the area of the Rudaki plains superposed on an MDIS mosaic of the region.

for regional studies.

Results: The global analysis updates earlier work [3], using all the MASCS observations available to date. The unsupervised hierarchical clustering of the global MASCS cube-image produces a tree of data partition, starting from two mega-regions. The first mega-region (MR1) comprises equatorial to mid-latitudes and the second (MR2) the two poles. The boundaries of MR2 at high northern latitudes approximate those of the volcanic northern plains [4]. MR2 areas show redder MASCS spectra than do MR1 areas.

A closer look in the area of the Rudaki plains reveals that a MASCS ratio map can show great variability on the scales on individual geological units (**Fig. 1**). Red areas on that map match closely to units inferred from images obtained with MESSENGER's Mercury Dual Imaging System (MDIS) [5, 6]. Parts of the Rudaki area (Calvino interior/surroundings and south of Rudaki) are similar to terrains extending southwest of Thakur. Bluer regions surrounding Thakur are correlated with the Homer-Kuiper region. The unsupervised hierarchical clustering produces a complete partitioning into regions differentiated by spectral characteristics. **Fig. 2** shows such partitioning for the Rudaki plains area. The central Rudaki plains and Calvino crater are spectrally associated with Thakur and part of its ejecta, as well as some pixels scattered in nearby areas (red in Fig. 2 and redder spectra). The plains themselves are separated into two large units (orange–green in Fig. 2, intermediate–red spectra). A fourth minor spectral unit (blue in Fig. 2, bluer spectra in this analysis) is strongly associated with Kuiper ejecta and Homer crater.

Conclusions: We have documented the presence of distinct spectral units on Mercury, as characterized by MASCS observations. The spectral units show some correlation with surface units mapped by MDIS. We have produced the first global hyperspectral data-cube image from normalized MASCS spectra. Data coverage varies by region, but global maps at 1 ppd can be obtained with at high ratios of signal to noise. Local areas can be analyzed at higher resolution, such as the Rudaki plains and their surroundings. The hierarchical clustering of these image cubes provides a representation of surface heterogeneities that is complementary to geological maps derived from MDIS. The same data will be integrated with newly available laboratory measurements of spectral reflectance [7], in support of geological and geochemical interpretations of MESSENGER observations [8,9].

References: [1] McClintock, W.E., et al. (2008), Science, 321, 92-94. [2] Izenberg, N.R., et al. (2008), Eos Trans. AGU, 89(53), Fall Meet. Suppl., abstract U11C-05. [3] D'Amore, M., et al., (2011), EPSC Abstracts, 6, EPSC-DPS2011-817 [4] Head, J.W. et al. (2011), Science, 333, 1853-1856. [5] Ernst, C.M., et al. (2010), Icarus, 209, 210-223. [6] Denevi, B.W., et al. (2009), Science, 324, 613-618. [7] Maturilli, A., et al. (2012), Lunar Planet. Sci., 43. [8] Helbert, J., et al. (2012), Lunar Planet. Sci., 43. [9] D'Incecco, P., et al. (2012), Lunar Planet. Sci., 43.

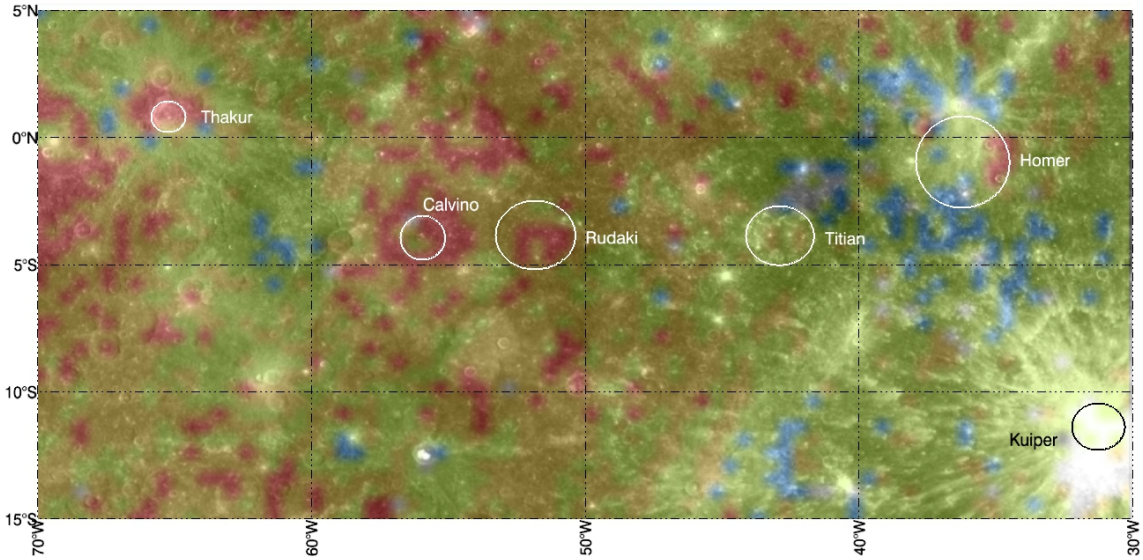

Fig. 2. Depiction of reflectance data clustering (see text) for the Rudaki plains area. Colors denote data clusters and are not intended to portray surface color variation.